MPHIL

Precision Spatiotemporal Water Sampling Autonomous Platform and Environmental Monitoring and Analysis System

Johnson, Tim

Award date:
2022

Awarding institution:
University of Bath

MPHIL

Precision Spatiotemporal Water Sampling Autonomous Platform and Environmental Monitoring and Analysis System

Johnson, Tim

Award date:
2022

Awarding institution:
University of Bath

THESIS

Precision Spatiotemporal Water Sampling Autonomous Platform and Environmental Monitoring and Analysis System

Submission by:
Tim Johnson

Supervisors:
Prof. Peter Wilson
Prof. Barbara Kasprzyk-Hordern

A thesis submitted in fulfilment of the requirements for the degree of Master of Philosophy

in the

Department of Electronic and Electrical Engineering

September 2020

Copyright Notice

Declarations

Declaration of any previous submission of the work

The material presented here for examination for the award of a higher degree by research has not been incorporated into a submission for another degree.

Candidate's signature

Declaration of authorship

I am the author of this thesis, and the work described therein was carried out by myself personally.

Candidate's signature

Acknowledgements

I would like to acknowledge, first of all, the invaluable advice and assistance provided by my lead supervisor, Prof. Peter Wilson. I would also like to thank Prof. Barbara Kasprzyk-Hordern for her helpful advice given in matters of chemical analyses.

A special thanks also to Dr. Zuhayr Rymansaib and Dr. Pejman Iravani, whose previous work on 3-D printed carbon electrodes at the University of Bath served as a helpful foundation for a part of my study.

Abstract

In an age where environmental concerns have become a common conversational topic, many freshwater sources still remain under-sampled and under-profiled both spatially and temporally, with respect to biological and chemical pollution. To this end, autonomous surface vehicles are excellent tools for the remote and autonomous monitoring of pollutants. The first objective of this study was to demonstrate how water sensors can be integrated onto an autonomous surface vehicle. This was accomplished by the mounting of a silicon (digital) temperature sensor onto a vehicle and programming the vehicle to conduct autonomous temperature measurements of the campus lake at the University of Bath. The second objective of this study was to develop a low-cost and portable heavy metals sensor. An inexpensive and compact PCB (printed circuit board) potentiostat was designed and pencil graphite electrodes were used for the determination of Zn^{2+} via differential pulse anodic stripping voltammetry (DPASV). This objective was partially satisfied; while the sensor and potentiostat were capable of measuring Zn^{2+} concentrations as low as 0.11g L^{-1}, conventional lab-based measurement techniques are able to measure concentrations of approximately 800μg L^{-1} (parts-per-billion range) and lower. While the designed sensor proved promising, further testing needs to be done using other types of electrodes in order to make accurate comparisons with the performance of conventional lab-based methods.

Contents

List of Figures

List of Tables

1 Introduction

1.1 Aim, Objectives, and Scope

The aim of my study was to work towards the development of an autonomous water sampling platform for real-time and remote environmental monitoring. This was achieved by building upon existing autonomous surface vehicle research already completed at the Department of Electronic and Electrical Engineering, where a freshwater platform already exists, allowing me to focus on water sampling and analysis.

The primary objective of the project was to develop water sensors capable of measuring specific chemical markers that correspond to various water quality parameters. I chose to pursue this objective by investigating sensors for the detection and measurement of heavy metal concentration in fresh water sources. The sensor was designed for the determination of Zn^{2+} concentrations; it comprises a PCB potentiostat and pencil graphite electrodes, uses the differential pulse anodic stripping voltemmetric (DPASV) method, and is controllable using the STM32-Nucleo-F302R8 micro-controller.

In investigating the sensors, I placed an emphasis on designing a "measurement rig" that is both portable and low-cost. Portability is an important trait as it allows the rig to be transported, with minimum fuss, into the field in order to conduct on-site and real-time sampling. A low overall cost, on the other hand, allows on-site sampling to be conducted without too much fear of damaging the rig since damaged components can be more easily replaced. Furthermore, a low overall cost would also allow the rig to be constructed and deployed in economically-poor regions.

2 Background

2.1 Water Sampling and Environmental Monitoring

Earth's many and abundant water resources, including lakes, rivers, coasts, and lagoons, play a critical role in sustaining life on the planet. Indeed, such is their importance that the recent increase in public concern regarding the environment has led to various efforts being undertaken to manage plastic pollution in these water resources. However, when it comes to chemical and biological pollution, a majority of these resources still remain vastly undersampled and under-profiled both spatially and temporally [11].

As such, the development of a robust solution that allows for the monitoring of these resources would bring about a number of benefits, with the primary advantage being the ability to develop a better understanding of water pollutants. This, in turn, allows for better pollution management, the long-term maintenance of ecosystem-based fisheries, and better conservation of marine life [12, 13]. It is also easier to conduct environmental impact assessments, on various human activities, in bodies of water that are well-profiled and well-sampled.

2.2 Water Quality Parameters

Turbidity and Colour

Two of the most obvious visual quality parameters of a body of water are its colour and turbidity. There are a number of factors that could cause a change in either parameter, including the presence of clay and silt particles, discharges of sewage or industrial waste, and the presence of large numbers of microorganisms [14]. As such, a change in either parameter could indicate the presence of pollutants.

Aside from their function as indicators of pollution, both colour and turbidity also affect the amount of light penetrating the body of water [15] and, thus, may have a significant impact on aquatic life. While it is near impossible to identify specific causes and pollutants through changes in either colour or turbidity, both remain useful water quality parameters as they can be measured easily and quickly using colorimetry or infrared (IR) spectroscopy methods.

Temperature

Thermal pollution, as a result of human activity, has been identified as a cause for concern since the mid-twentieth century [16], and is known to negatively affect water quality and aquatic life. It is primarily caused by power plants and industrial reactors, where water is used as a coolant and discharged at temperatures above the ambient temperature [17]. The result of this, according to a recent study [18], can be seen in notable rivers such as the Rhine, which experiences an average temperature increase of $\geq$ 5℃ throughout the year. It can also be caused, albeit to a lesser degree, by urban run-off during warm weather, in which storm water passes over hot urban land areas and flows into streams, rivers, and lakes.

Nitrogen and Phosphorus

Nitrogenous compounds (in the form of nitrates, nitrites, ammonia, and organic nitrogen) and phosphorus compounds (in the form of insoluble phosphates) may originate from a number of sources, the largest being human sewage, both raw and treated. Other sources include geological erosions, nitrogen fixation carried out by algae and aquatic plants, washout of NO_x compounds from the atmosphere, and agricultural fertilizer run-offs [19].

Excessive levels of nitrogenous and phosphorous compounds are often associated with eutrophication, plant overgrowth, and harmful algal blooms due to the role of both compounds as nutrients for plants and algae [19]. This has a significant effect on dissolved oxygen (DO) concentration as plant photosynthesis may cause excessive DO levels during the day and respiration may cause severely low DO levels at night. Furthermore, overgrowths of plants and algae will cause an increase in the concentration of bi-carbonate ions, a by-product of photosynthesis, driving up the pH.

Ammonia is also of concern as it is toxic to most aquatic organisms, because they lack the mechanism to prevent its build-up in the bloodstream [20].

pH

The pH of a body of water is another key factor involved in sustaining aquatic life as many biological activities tend to operate within a limited pH range of 5-8 [14]. Under most circumstances, a change in pH is likely to only cause a localized effect in oceanic bodies of water due to the natural buffering capacities of seawater [19]. This may not be the case in freshwater sources, however, where an increase in sulphur and nitrogen concentrations may severely depress pH levels to as low as pH 4. On the other hand, an increase in the concentration of bi-carbonate ions, a by-product of photosynthesis, may significantly increase pH levels to beyond pH 10.

Organic Material/Degradable Wastes

According to Clark [19], most of the pollutants entering coastal waters are composed of organic materials, originating from urban sewage, agricultural wastes, food processing wastes, oil spillages, chemical wastes, etc. The organic materials are broken down over time, mostly by aerobic bacterial action, into inorganic compounds such as carbon dioxide, water, and ammonia. This is an oxidative process, which means that oxygen is consumed as the materials are degraded [19].

If there is a large enough input of organic materials, the rate of oxygen consumption may exceed the DO supply, causing deoxygenation. In a deoxygenated environment, further degradation will depend on anaerobic bacterial action, which is slow and yields more undesirable end-products such as methane and hydrogen sulphide [19].

The presence of organic material is often quantified by measuring either the chemical oxygen demand (COD) or the biochemical oxygen demand (BOD). The BOD is the amount of DO that is needed to breakdown, via bacterial action, the organic materials present in a water sample at a certain temperature over a specific time period. The COD is similar to the BOD but less specific, and is the amount of oxygen needed for all oxidising reactions in a water sample.

Heavy Metals

There are a wide range of naturally occurring metals in many water sources, mainly due to the weathering of minerals [21]. However, anthropogenic activities such as mining and quarrying has caused an increase in the concentration of heavy metals in many rivers [21]. This is of concern as heavy metals are non-degradable and often considered very toxic and damaging to the environment.

One example of this is zinc, which is a common pollutant associated with the mining of coal, lead, silver, and a number of other metals. Even at relatively low concentrations, it is considered toxic to many aquatic organisms [22]. Other heavy metal pollutants that can cause severe damage to the environment include mercury, cadmium, copper, lead, tin, iron, arsenic, silver, and nickel [19].

Microbial Population

The monitoring of certain aquatic populations of bacteria, viruses, and parasites may be useful for the detection of pathogens, especially in waters that are used for recreation or as sources of drinking water. One of the most commonly monitored species of bacteria is *Escherichia coli* (also known as *E. coli*), which is a reliable indicator of human and animal faecal contamination [23]. Although *E. coli* is not normally considered pathogenic in natural waters, it is frequently accompanied by pathogens such as viruses [24].

Some populations of phytoplankton, such as cyanobacteria, dinoflagellates, and diatoms, may form harmful algal blooms when over-populated. This is often the result of an over-abundance of nutrients in the water. These algal blooms deplete DO levels, reduce sunlight penetration, and may even create "dead zones" where neither fish nor plants can survive [25]. Harmful algal blooms may also produce potent toxins that, when ingested, can be fatal to humans, land animals, sea mammals, birds, and fish [26].

2.3 Autonomous Surface Vehicles

With the currently growing interest in the monitoring and analysis of water pollution, there is also a need to increase the quantity and precision of data available, both spatially and temporally [12]. The availability of such an archive of data would enable scientist to not only develop a better comprehension of individual bodies of water, but also build an understanding of the behaviour of pollutants with respect to drift over time, seasonal variations, anthropological activities, weather events, water levels, and their links to phenomena such as algal blooms and spillages.

The use of a mobile sampling platform for remote sensing and sampling allows greater flexibility than the current convention of using fixed platforms and sensors [27]. The platform could be a game-changer as it would greatly expand the number of possible sampling locations. The possibility of measuring and analysing water samples in-situ would also speed up the time needed to profile bodies of water.

Another key challenge in the field of water sampling and analysis is that current sampling and monitoring methods, due to human error, lack the consistency in sample location, time, or quality. By using an autonomous sampling platform, the human error aspect can be eliminated, allowing for greater consistency in the gathering of water samples.

A number of Autonomous Surface Vehicles have already been developed over the past two decades for a variety of purposes. The **SCOUT** (Surface Craft for Oceanographic and Undersea Testing) kayak, developed at the Massachusetts Institute of Technology, has a hull made of HDPE (high density polyethylene) and is designed to accommodate a range of payloads for the collection of hygrographic data [28].

The **DELFIM** catamaran was designed by the *Instituto Superior Técnico* (Portugal) to collect marine data, and to serve as a support vessel [29]. The **Measuring Dolphin** catamaran, built by the University of Rostock (Germany), is capable of high accuracy positioning and track guidance, and carrying hygrographic sensors [30].

The **Springer** (University of Plymouth), the **Wivenhoe** (CSIRO Autonomous Systems Laboratory, Australia), and the **Lizhbeth** (University of Zurich, Switzerland) catamarans were designed for the monitoring and tracing of pollutants [31, 32, 33]. The **Charlie** catamaran was built by the CNR-ISSIA Genova (Italy) for the collection of sea surface microlayers [34].

Table 1: Autonomous surface vehicles developed over the past two decades

Autonomous Surface Vehicles	Year	Function
DELFIM [29]	2000	Acoustic relay
SCOUT [28]	2005	Collection of hygrographic data
Measuring Dolphin [30]	2006	Collection of hygrographic data
Springer [31]	2006	Monitoring of water pollutants
Charlie [34]	2008	Collection of sea surface microlayers
Wivenhoe [32]	2010	Monitoring of water pollutants
Lizhbeth [33]	2013	Monitoring of water pollutants

2.3.1 The Autonomous Water Sampling and Monitoring Platform

The Autonomous Surface Vehicle that has been developed at the University of Bath's Department of Electronic and Electrical Engineering is a catamaran with foam-based hulls, designed to be able to accommodate interchangeable payloads. It has two BlueRobotics T100 thrusters, one mounted in the back of each hull, and is fitted with aluminium struts for holding in place the payload and other installed components. The thrusters are powered by two LiPo 3s 11.1V 1.5A batteries.

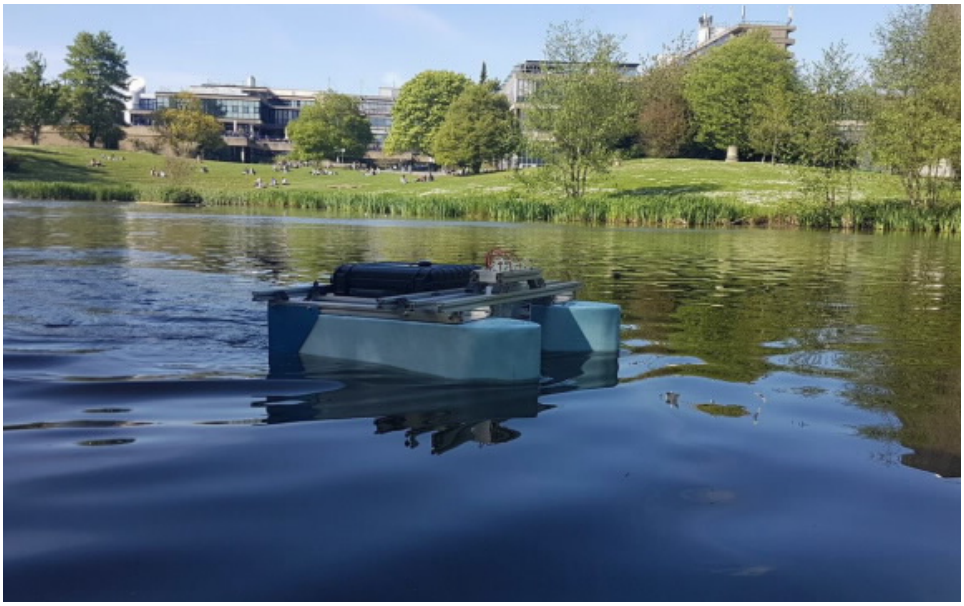

Figure 1: The Autonomous Surface Vehicle developed at the Department of Electronic and Electrical Engineering

The Pixhawk Board

The control of the navigational functions of the vehicle was accomplished by using a Pixhawk board, the set-up for which is given below. The Pixhawk is an "off-the-shelf" high-performance flight controller, capable of providing control and automation for a variety of vehicles, including fixed-wing and multi-rotor drones, helicopters, rovers, and boats. It has an internal compass and accelerometer, and can connect to a maximum of 14 PWM outputs.

Table 2 lists the specifications of the Pixhawk board, while Figure 2 presents the layout of the Pixhawk interfaces [8].

Table 2: Pixhawk board - specifications [8]

Processor	32-bit STM32-F427 ARM Cortex M4 core with FPU
	168 Mhz / 256 kB RAM / 2MB Flash
	32-bit STM32-F103 failsafe co-processor
Sensors	Invensense MPU6000 3-axis accelerometer/gyroscope
	STM L3GD20H 16-bit gyroscope
	STM LSM303D 14-bit accelerometer
	MEAS MS5611 barometer
Power	Ideal diode controller with automatic failover
	Servo rail high-power (max. 10V) and high-current (10A+) ready
	All peripheral outputs over-current protected, all inputs ESD protected
Interfaces	5× UART (serial ports), one high-power capable, 2 with HW flow control
	Spektrum DSM / DSM2 / DSM-X Satellite compatible input
	Futaba S.BUS compatible input and output
	PPM sum signal input
	RSSI (PWM or voltage) input
	I2C, SPI, 2× CAN, USB
	3.3V and 6.6V ADC inputs

Figure 2: Pixhawk interfaces layout

Mission Planner

Mission Planner is a free, open-source, Windows-compatible software, supported by ArduPilot, that functions as a ground control station for the Pixhawk board. It can be used to both configure the Pixhawk board and as a dynamic control supplement for the autonomous vehicle. It also allows for easy plotting of waypoints for autonomous missions using an on-screen map and a "point-and-click" system.

When configured with appropriate telemetry hardware, the software is also capable of displaying the status of the vehicle while in operation. Figure 3 shows the user interface of the Mission Planner software.

Figure 3: User interface of the Mission Planner software

The Radio Control System

Manual steering of the vehicle is achieved using a FlySky T4B 4-channel controller-receiver set. This allows the vehicle to be steered manually, especially in cases where a GPS lock cannot be acquired or where the use of the auto-piloting system is not feasible.

Overall Setup

The electronic components required for the control of navigational functions were connected to the Pixhawk board. The left and right thrusters were connected to "Main Output 1" and "Main Output 3" respectively. An external

GPS module was connected to the "GPS" and "I2C" ports, a buzzer was connected to the "Buzzer" port, and a safety switch (functioning as a physical arm/disarm button) to the "Switch" port. The radio control receiver was connected to the "RC In" port via a PPM encoder.

In order to be configured, the Pixhawk board was connected via USB to the Mission Planner application. The latest ArduRover firmware, which is used for rovers, boats, and ground vehicles, was downloaded and installed on the board. The compass, accelerometer, radio controller, and flight modes were then configured and calibrated with the aid of the Mission Planner application.

Once the firmware had been installed and the individual components have been properly configured and calibrated, the next step was to modify a few configuration parameters by navigating to "Config/Tuning →Full Parameter List". Table 3 contains a list of the configuration parameters that were modified. Finally, a FPV radio telemetry set was configured to allow remote communications between the Pixhawk board and the Mission Control application.

Table 3: Pixhawk Configuration Parameters

Configuration Parameter	**Value**
FRAME_CLASS	2 (boat)
PILOT_STEER_TYPE	1 (two paddles input)
SERVO1_FUNCTION	73 (throttle left)
SERVO3_FUNCTION	74 (throttle right)

2.4 Temperature Sensing

As discussed above, thermal pollution is one of the many key parameters that need to be monitored for the purpose of water quality assurance. This section presents a literature review of the various mainstream temperature measurement techniques, followed by the selection and design of a simple temperature sensor to be used, with the Autonomous Surface Vehicle, for autonomous temperature measurement.

Temperature sensors usually operate by detecting a change in a physical parameter, such as resistance or voltage, and using an empirical correlation to determine temperature. In general, temperature sensors can be either contact or non-contact.

Platinum Resistance Temperature Detector (RTD)

One of the most commonly used temperature sensors in the bioprocess industry is the platinum resistance temperature detector (RTD) [35]. To measure temperature, RTDs rely on the use of a resistance wire, which has a precise resistance-temperature relationship, wound on a suitable former [36]. The resistance wire typically comprises a metal with a positive temperature coefficient; this is most commonly platinum, nickel, tungsten, or copper [1]. Platinum is the preferred material due to its superior accuracy, predictability, and stability compared to the other materials[1]. Furthermore, platinum has a much higher useful temperature range (approx. -270℃ to 650℃) than the other materials, while also possessing a highly linear resistance change [9].

Advantages [1]:

- Excellent accuracy and repeatability
- Relatively wide operating temperature ranges
- Low drift over time
- Linear resistance-temperature curves. Figure 4 shows an example of this.
- Standardised resistance-temperature properties, meaning they are highly interchangeable

Disadvantages [1, 9]:

- Higher cost than most other temperature sensors due to the materials used
- Resistive devices undergo a self-heating effect which may compromise system accuracy, depending on the mass and thermal conductivity of the device

Table 4: Typical operating temperatures of common RTD element materials [9]

Material	Operating Temperature Range
Platinum	-270 to 650℃
Nickel	-100 to 315℃
Copper	-75 to 150℃
Nickel/Iron	0 to 205℃

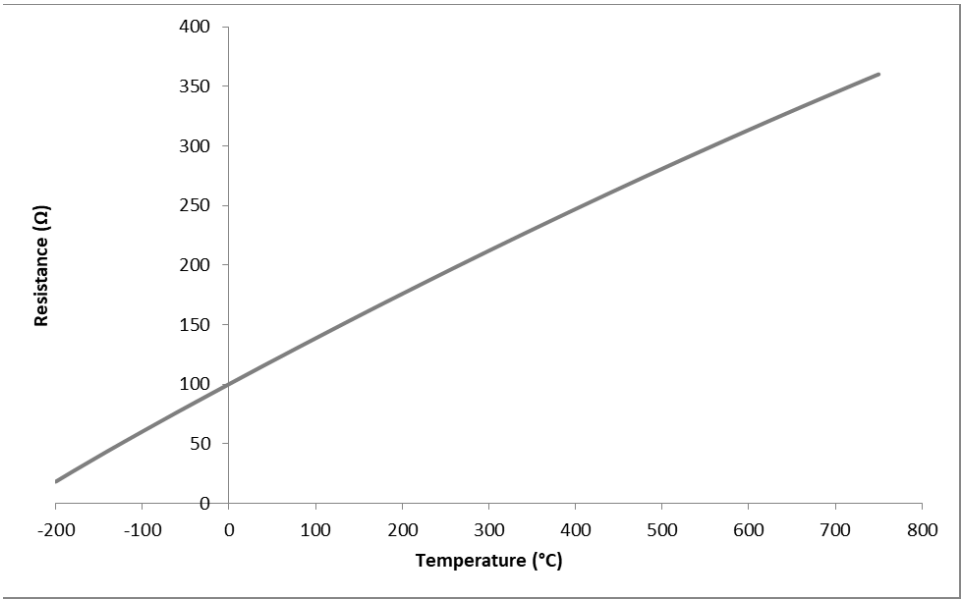

Figure 4: Resistance-temperature curve of a thin-film platinum RTD (ice-point resistance = 100Ω) [1]

Thermistor

Thermistors, like RTDs, rely on materials whose resistances are temperature-dependent in order to measure temperature, and are classified as either positive temperature coefficient (PTC) or negative temperature coefficient (NTC). For PTC thermistors, resistance increases with temperature; NTC thermistors, on the other hand, display a decrease in resistance as temperature increases. Thermistors are typically constructed using a combination of metal oxides sintered to a ceramic base while PTC thermistors can also be made from conductive polymers [1].

Advantages [1]:

- Relatively low cost, since they do not utilise expensive pure metals such as platinum
- The most sensitive to changes in temperature, compared to other sensors

Disadvantages [1, 36]

- Non-linear resistance-temperature curves, so their operation is limited to a narrow temperature range to minimise non-linearity
- Lower exposure temperatures compared to RTDs and thermocouples

because their stability is adversely affected by long-term exposure to high temperatures

- May fail closed, producing a resistance that can be wrongly interpreted as a temperature reading
- Like RTDs, thermistors may also struggle with self-heating which affects measurement accuracy
- Non-standardised resistance-temperature properties, so they are not very interchangeable; resistance-temperature data is usually supplied by the respective manufacturers

Thermocouple

Thermocouples consist of two electro-conductive wires, made from different metals or alloys, that are connected at one end of a circuit [9]. The two ends of the conductors are known as junctions. The end of the conductors that is exposed to the process temperature is referred to as the measurement (hot) junction. The other end is known as the reference (cold) junction and is maintained at a known reference temperature. When the temperature at two junctions are different, a temperature-dependent millivolt potential is formed within the conductors [36]. The magnitude of this potential, along with a knowledge of the reference temperature and the type of thermocouple used, can then be used to determine the temperature at the measurement junction.

Advantages [9]:

- Largest operating temperature range compared to other sensing technologies
- Relatively low-cost, due to their simple design
- Highly durable, can be deployed in many environments

Disadvantages [9, 1]:

- The exposed measurement junction is often susceptible to corrosion and oxidation
- The use of a thermowell or stainless steel sheath to shield the measurement junction will result in slower thermal response times, lower accuracy, and higher susceptibility to electromagnetic interference
- Less stable than other sensors at moderate to high temperatures

Silicon Temperature Sensor

Silicon sensors operate by taking advantage of the bulk electrical resistance properties of semi-conductive materials, with resistance increasing almost linearly with temperature at low temperatures [1]. They are highly sensitive, are typically available for operating temperatures that range from cryogenic to about 200℃ [1], and are used extensively in integrated circuits (IC).

Advantages [1]:

- Highly linear resistance-temperature curves
- Cheaper than RTDs
- Suitable for low-temperature operation

Disadvantages [1]:

- Resistance-temperature curves are less linear than that of RTDs
- Less accurate, longer thermal response times, limited operating temperature ranges compared to RTDs, thermistors, and thermocouples
- More costly than thermistors and thermocouples

General Considerations and Comparisons

For the selection of temperature sensors, one key parameter that has to be considered is the operating temperature range; a comparison of the typical operating ranges of each type of sensor is listed in Table 5.

Table 5: Operating ranges of different temperature sensors [1]

Temperature Sensor	Operating temperatures
RTDs	-273.15 to 200℃
Thermistors	-100 to 500℃
Thermocouples	-200 to 2315℃
Silicon sensors	-273.15 to 200℃

The tolerance, accuracy, and sensitivity of the measurements of each sensor should also be taken into consideration. Tolerance is the total allowable error within a system, typically given as plus or minus a particular temperature. Accuracy, on the other hand, is the ability of the sensor to measure the true value of the temperature over a temperature range [9]. Depending on their design, RTDs, thermistors, thermocouples, and silicon sensors are all capable of maintaining tolerances of less than ±1.7°C, while RTDs generally give the best overall accuracy compared to other sensors [1].

When considering sensitivity, the thermal inertia of the sensor needs to be taken into account; this is a function of the mass of the sensor as well as the thermal conductivity of the material used. A summary, including the general attributes of each type of sensor, can be found in Table 6.

2.5 Heavy Metals Sensing

Another important parameter for the monitoring of water quality is the concentration of heavy metals. While atomic absorption spectrometry, inductively coupled plasma - atomic emission spectroscopy (ICP-AES), and inductively coupled plasma - mass spectrometry (ICP-MS) are all techniques that have been proven to be highly reliable for the determination of trace metals, they are ill-suited for remote and autonomous monitoring of heavy metals in water. This is mostly due to these techniques being relatively expensive, both in terms of resources and equipment, and the need for highly-trained technicians for the operation of said equipment [7]. The equipment required for these techniques also tend to be rather bulky and cannot be easily transported into the field for in-situ measurement.

Recently, there has been a growing trend towards the use of electrochemical techniques, such as voltammetry, for the measurement of heavy metals concentration in water. Yantasee *et. al.*, for example, suggest that anodic stripping voltammetry could be a highly desirable technique because of its high detection sensitivity, which is "due to the combination of the built-in pre-concentration step with powerful voltammetric techniques that generate an extremely favourable signal-to-noise ratio" [37]. Previous studies have also shown anodic stripping voltammetry techniques to be economic and easily used by personnel with minimal training [37, 7, 38, 39].

This subsection will present an overview of common voltammetric techniques currently in use, and their applications.

Table 6: General attributes of each temperature sensor

Sensor	Advantages	Disadvantages
RTD	• Great accuracy and repeatability • Excellent stability • Interchangeable • Linear resistance-temperature curves	• Bulkier than other sensors • More costly than other sensors
Thermistor	• Greatest sensitivity • High resolution • Short thermal response times • Relatively cheap	• Non-linear resistance-temperature curves • Limited operating temperature range • May struggle with self-heating
Thermocouple	• Widest operating temperature range • Low cost • Excellent durability • Can operate at extremely high temperatures	• Susceptible to corrosive environments • Less stable than other sensors at mid to high temperatures
Silicon sensor	• Cheap • Linear resistance-temperature curves	• Limited operating temperature range • May experience self-heating

2.5.1 Basic Theory

The common underlying principle behind all voltammetric techniques is that they involve applying a potential (E) to an electrode and monitoring the resulting current(i) that flows through the electrochemical cell. In most cases, it is desirable to either vary the applied potential or to monitor the current over a period of time (t) [40].

Most voltammetric techniques employ a three-electrode arrangement, comprising a working electrode, a counter electrode, and a reference electrode. The working electrode serves as the site at which the redox reactions take place during analyses. the counter electrode allows current to flow to and from the working electrode, and is usually made from an inert material, such as platinum, gold, graphite, or glassy carbon, and does not participate in the electrochemical reaction.

The reference electrode is a stable electrode with a well-known, constant potential. It is used as a point of reference in the cell for the control and measurement of the potential applied on the working electrode. Typical reference electrodes for aqueous solutions are the saturated calomel electrode (SCE) and the silver/silver chloride electrode (Ag/AgCl). Ideally, there should be no current flow through this electrode.

General advantages of voltammetric techniques [40]:

- Excellent sensitivity
- A very wide useful linear concentration range (10^{-12} to $10^{-1}M$) for both organic and inorganic species
- Analysis times can be as short as mere seconds
- Several analytes can be determined simultaneously
- A wide range of useful solvents and electrolytes

2.5.2 Polarography

Polarography can be said to occupy a special place in history because its discovery by Jaroslav Heyrovsky in 1922 marked the beginning of the field of voltammetry. It is also rather unique due to its use of a dropping mercury electrode (DME) as a working electrode, which consists of a succession of mercury drops flowing, under gravity, through a glass capillary [40]. As the drop grows, the current increases with increasing area; conversely, as the drop falls, the current also falls. Each new drop also provides a clean surface for the redox process to take place. Figure 5 below shows a polarogram,

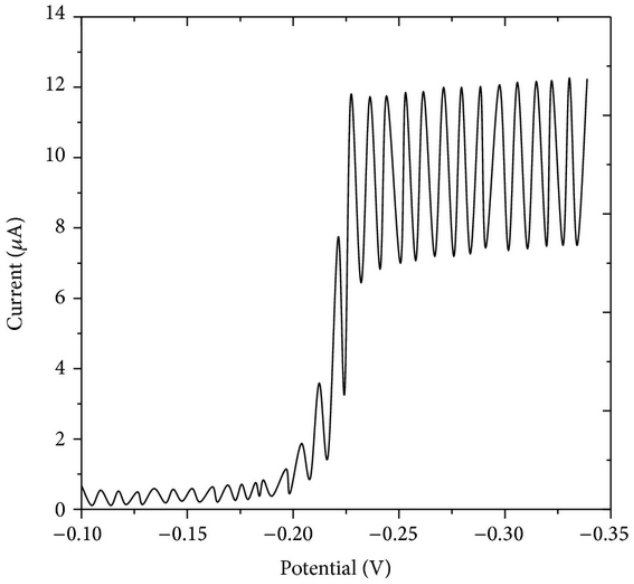

Figure 5: Example of a typical polarogram [2]

where the effects of the growth and falling of each drop can be seen. The plateau current is proportional to the concentration of the analyte, while the half-wave potential, which is the potential when the current is half the value of the plateau current, is specific to the analyte's matrix [40].

The polarography technique has several disadvantages that can limit its usefulness. Chief among these is that mercury is oxidised at potentials more positive than +0.2V versus SCE [40], making analyses in the positive potentials impossible. Another disadvantage is that the charging of the electrode surface, which has a large capacitance, causes residual currents which may skew the current readings.

2.5.3 Cyclic Voltammetry (CV)

Although rarely used for quantitative applications, cyclic voltammetry (CV) is often found to be useful for the study redox processes, for understanding reaction intermediates, and for obtaining stability of reaction products [40]. Cyclic voltammograms are produced by monitoring the current while varying the applied potential at the working electrode in both the positive and negative directions, at a fixed scan rate.

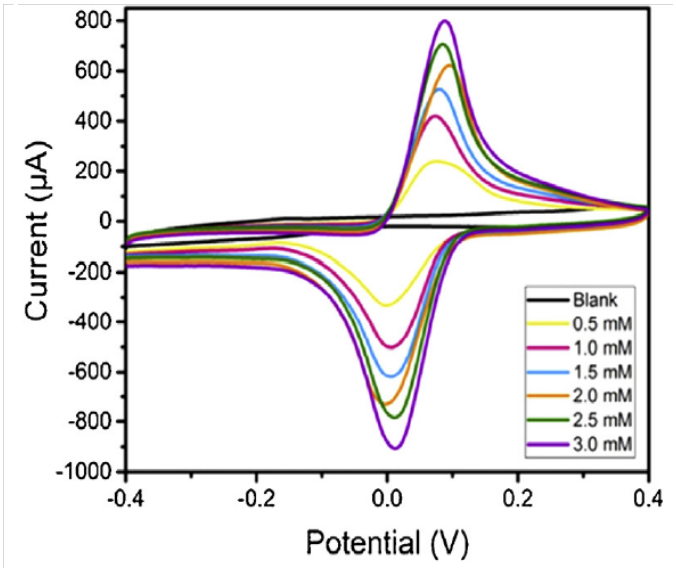

Figure 6: Example of a cyclic voltammogram of various p-aminophenol concentrations [3]

CV tends to employ a three-electrode arrangement (working, counter, and reference electrodes) and is usually carried out in a quiescent solution. Although mercury film electrodes are traditionally favoured, glassy carbon, platinum, gold, graphite, and carbon paste are all suitable working electrodes [40].

2.5.4 Pulse Methods

Pulse voltammetric methods were developed with an eye on increasing the speed and sensitivity of the measurements. These techniques employ a form of potential modulation, instead of a simple staircase ramp, when scanning the applied potential in either direction. The three most commonly used methods are normal pulse, differential pulse, and square-wave voltammetry.

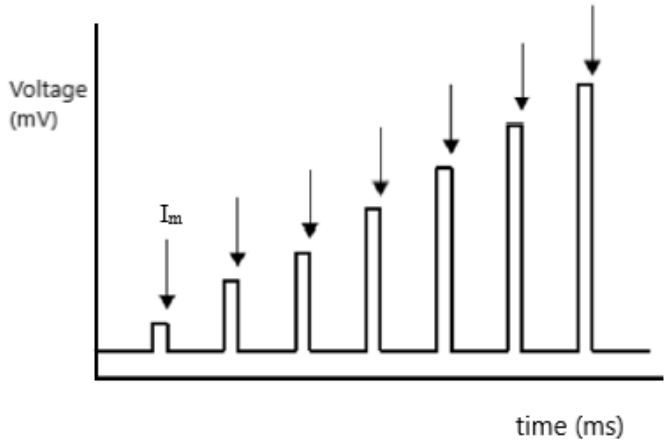

Figure 7: Example of the normal pulse waveform used for NPV [4], where I_m is the point at which current is measured for each pulse

Normal Pulse Voltammetry (NPV) involves the use of a series of potential pulses of increasing amplitude, starting at an initial potential, E_i. Each pulse has a fixed duration, τ, of approximately $1 - 100$ms and the interval between pulses is set at around $0.1 - 5$s [40]. The current is measured near the end of each pulse. The voltammogram is obtained by plotting the measured current (y-axis) against the potential to which the pulse is stepped (x-axis).

Differential Pulse Voltammetry (DPV) differs from NPV in that the amplitude of the potential pulses is fixed, typically at around $10 - 100$mV [40]. The pulses, however, are superimposed on a slowly changing base potential. Current is sampled twice per pulse: the first measurement, i_1, is made just before the pulse is applied and the second, i_2, at the end of the pulse. The voltammogram is obtained by plotting the current differential $(i_2 - i_1)$ against the base potential.

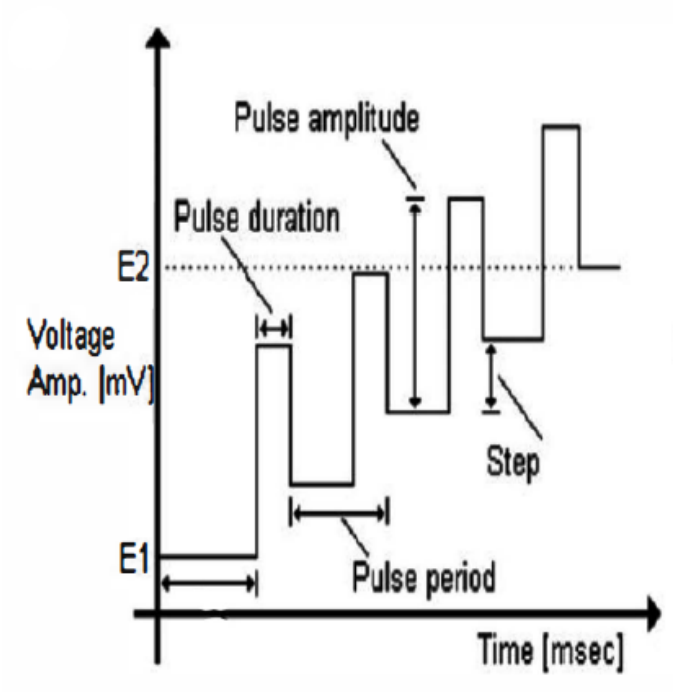

Figure 8: Example of the differential pulse waveform used for DPV [5]

Square Wave Voltammetry (SWV) uses a staircase waveform with a fixed step height and symmetrical square-wave pulses with a fixed amplitude (ΔE_p) superimposed on the waveform, so that the forward pulse of the square wave coincides with the staircase step. The voltammogram is obtained by plotting the net current ($i_{\text{net}} = i_{\text{forward}} - i_{\text{reverse}}$ - see Figure 9) against the stepped potential (ΔE_s), with the peak centred on the redox potential of the analyte and peak height directly proportional to analyte concentration.

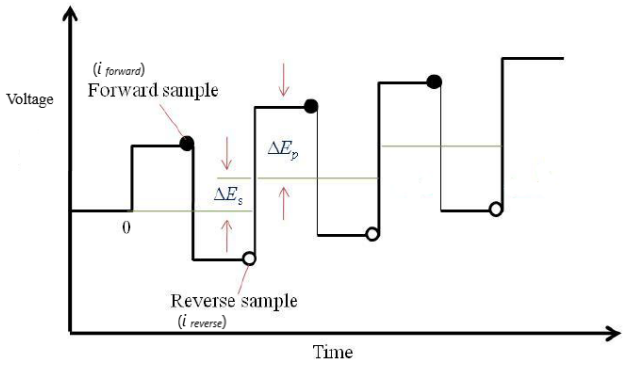

Figure 9: Example of the square-wave waveform used for SWV, where i_{forward} and i_{reverse} are points at which current is measured, ΔE_s = step height, and ΔE_p = pulse amplitude [6]

2.5.5 Deposition and Stripping Techniques

Deposition and stripping techniques are often credited with having the very low detection limits when compared to other electroanalytical techniques [40]; this is mostly due to the pre-concentration (or deposition) step, where the analyte species in the sample solution is deposited onto the working electrode. During the subsequent stripping step, the analyte is stripped from the working electrode using a potential scan and the current is measured. The stripping of the analytes produce peak currents (i_p), which are proportional to the concentration of each analyte, at different peak potentials (E_p), which are specific to each analyte.

It is possible to use a variety of waveforms during the stripping step (*e.g.* linear sweep, differential pulse, square-wave, staircase), although square-wave and differential pulse waveforms are mostly favoured [40]. The three most commonly used methods are anodic stripping voltammetry (ASV), cathodic stripping voltammetry (CSV), and adsorptive stripping voltammetry (AdSV).

Anodic Stripping Voltammetry (ASV) is used extensively for the detection of trace metals, and has the advantages of having a very low detection range (parts-per-trillion) and the ability to measure multiple analytes simultaneously [40]. During the deposition step, a negative potential is applied to the working electrode, causing metal ions in the sample solution to be reduced and deposited onto the surface of the working electrode. The metals are then stripped (or oxidised) away by scanning the applied potential in the positive direction.

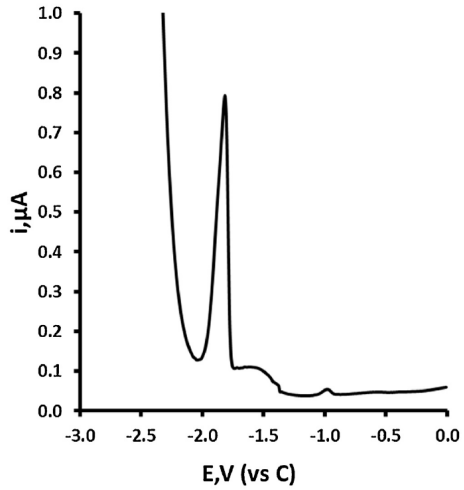

Figure 10: Typical voltammogram obtained by Honeychurch *et al* (2018) for the determination of Zn^{2+} via Anodic Stripping Voltammetry [7]

Cathodic Stripping Voltammetry (CSV) is normally used to measure specific ionic species that tend to form insoluble salts at the anode. CSV functions similarly to ASV, except that a positive deposition potential is applied to the working electrode and the potential is scanned in the negative direction during the stripping step.

Adsorptive Stripping Voltammetry (AdSV) is different from both ASV and CSV in that the analyte is not deposited on the working electrode by accumulation via electrolysis. Instead, deposition is achieved through adsorption on the electrode surface or by specific reactions using chemically-modified electrodes.

2.5.6 Electrodes

The electrodes for the voltammetric cell are also subject to the same requirements as the potentiostat, in terms of cost and portability. Most of the commonly used electrodes, however, have to be excluded from consideration as they are relatively expensive and are generally unsuitable for in-situ determination of trace metals in fresh water sources. For example, mercury-based electrodes cannot be used since mercury itself is a heavy metal pollutant. Exposing these costly electrodes directly to polluted waters is also undesirable as the electrodes may foul up or get damaged.

Previous studies have suggested carbon- and graphite-based electrodes as suitable alternatives to the conventional electrodes used for voltammetry [41, 42, 43, 7]. In particular, pencil graphite electrodes have been shown to be good, low-cost alternative electrodes for the detection of trace metals via stripping voltammetry [44, 45, 46]. For this reason, and the fact that graphite is chemically inert with respect to redox reactions, pencil graphite electrodes were used in this study for both the working and counter electrodes. A graphite pseudo-reference electrode was used in place of the usual reference electrode, as demonstrated by Honeychurch *et. al.* [7].

The pencil graphite electrodes were extracted from Staedtler Noris HB pencils by carefully splitting apart the wooden sleeve and polishing the surface of the pencil graphite on tracing paper.

3 Temperature Sensing

3.1 Design of a Temperature Sensor

In selecting an appropriate type of temperature sensor for the system, a few things have to be taken into consideration. Firstly, the sensor should be relatively low cost in order to maintain the feasibility of the project. It should be able to operate underwater at a temperature range of about -10 to 40℃, which should encompass the possible range of UK surface water temperatures. It should also be fairly sensitive, so as to accurately capture any spatial and temporal variations in water temperature.

The temperature sensor selected was a Maxim DS18B20 digital temperature sensor, which is a silicon-based sensor packaged in a waterproof environment. Its features are listed in Table 7. A silicon sensor was chosen because of its low cost and linear resistance-temperature curve. The limited operating temperature range of silicon sensors is not of any concern since, in this case, the measured temperatures will be close to ambient and in a fairly narrow range.

Table 7: DS18B20 digital temperature sensor features [10]

Feature	DS18B20
Price	1 - 3£
Supply Voltage	3.0 - 5.5V (DC)
Accuracy	±0.5℃within -10 to 85℃
Operating range	-55 to 125℃

Figure 11: DS18B20 digital sensor with Pin Configuration

The DS18B20 comes pre-calibrated to provide 9-bit to 12-bit Celsius temperature measurements. It uses a "1-Wire bus", which means that only one data line (and ground) is needed to communicate with a micro-processor [10]. Furthermore, each DS18B20 possesses a unique 64-bit serial code; this means that multiple DS18B20s to function on the same "1-Wire bus", allowing one micro-processor to control multiple DS18B20s at the same time [10].

The DS18B20 comes pre-calibrated to provide 9-bit to 12-bit Celsius temperature measurements. It uses a "1-Wire bus", which means that only one data line (and ground) is needed to communicate with a micro-processor [10]. Furthermore, each DS18B20 possesses a unique 64-bit serial code; this means that multiple DS18B20s to function on the same "1-Wire bus", allowing one micro-processor to control multiple DS18B20s at the same time [10].

3.2 Integration of the Temperature Sensor with the Autonomous Surface Vehicle

The design of a real-time remote temperature-sensing platform using the Autonomous Surface Vehicle, while a relatively simple task, is a useful demonstration of the capabilities of the vehicle and can provide a helpful indication of how other sensors can be integrated onto the platform.

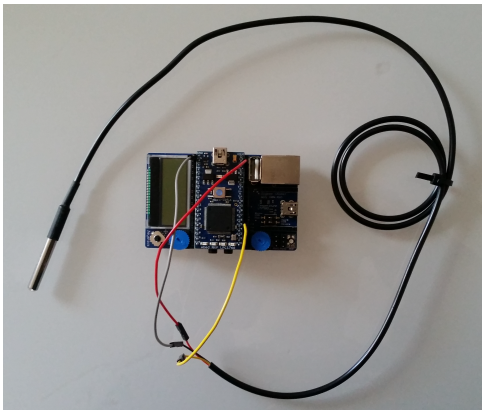

Figure 12: DS18B20 temperature sensor connected to the mbed LPC1768 board

I constructed a simple test-run at the university's lake by mounting the payload, containing the DS18B20 temperature sensor, onto the Autonomous Surface Vehicle and plotting a number of waypoints onto the on-board navigational system (controlled by the Pixhawk board). The vehicle was programmed, using the Mission Planner application, to carry out its mission autonomously, loitering at each waypoint for 30 seconds in order to gather surface temperature readings. Figure 13 provides a visual representation of the waypoints plotted for the test-run, while Figure 14 shows a chart of the lake surface temperature, plotted using MATLAB, based on the measured values.

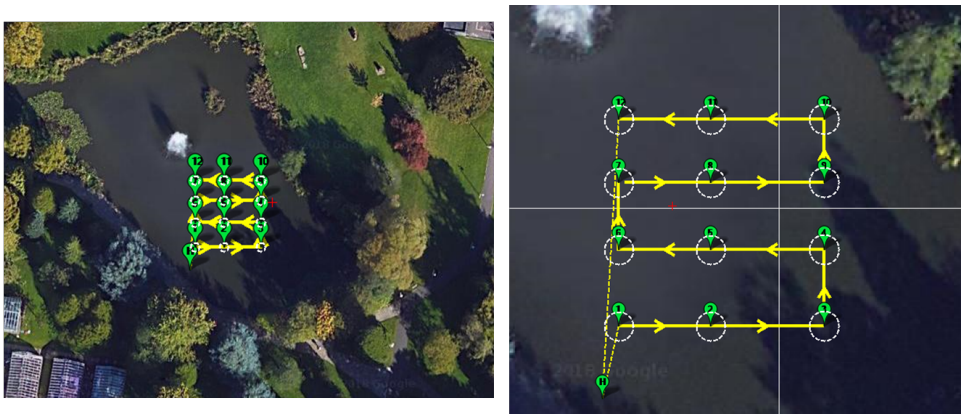

Figure 13: The plotted waypoints for the test-run at the university's lake

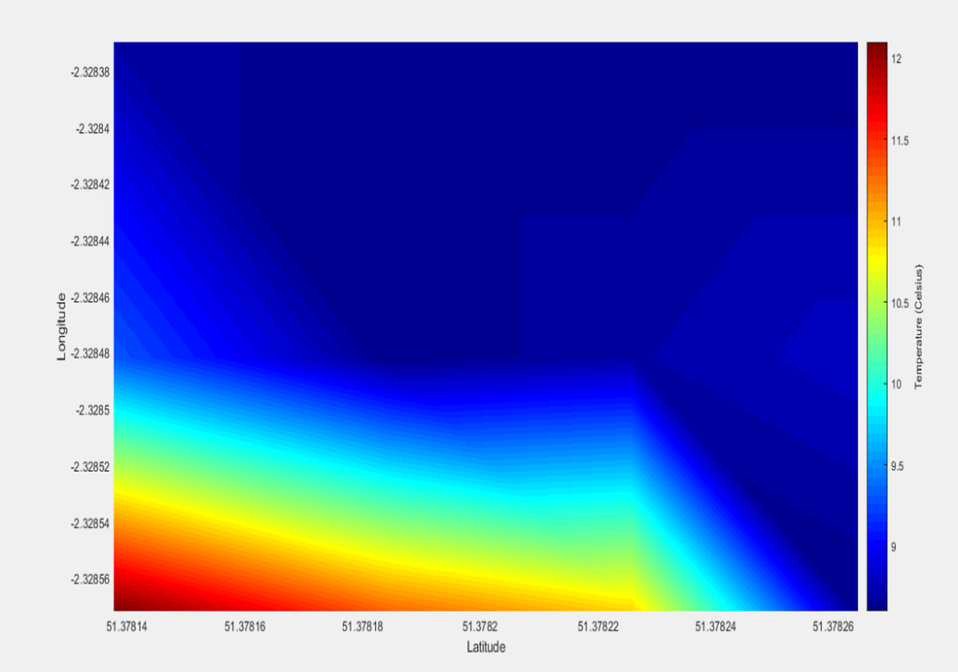

Figure 14: Surface temperature chart of the university's lake based on the measurement values at each plotted waypoint

3.3 Conclusions and Further Considerations for Future Designs

This simple test-run at the university's lake demonstrates the ease with which sensors can be integrated onto the Autonomous Surface Vehicle. One main consideration, however, is the length of time the vehicle spends loitering at each waypoint. This is, of course, highly dependant on the sensitivity of the sensor, as a sensor that is more sensitive to change would require a shorter time to "adjust" to its new location and obtain an accurate reading. Therefore, when programming a mission for the Autonomous Surface Vehicle, the loitering time should be long enough to ensure more accurate readings.

4 Heavy Metals Sensing

4.1 Design of a Novel Heavy Metals Sensor

In order to achieve the aim and objectives outlined in Section 1.1, the design of a sensor capable of measuring the concentration of heavy metals in water has to take into account both the cost and portability of the sensor, while

still maintaining a reasonable level of sensitivity. Portability is a necessary trait to enable remote and autonomous sensing, using the autonomous surface vehicle discussed in Section 2.3.1. A low-cost sensor can be easily replaced if it is damaged while conducting in-situ measurements, and also allows the sensor to be deployed in economically-poor regions.

4.1.1 Potentiostat Design

In voltammetry, the potentiostat is the instrument tasked with applying a potential to the working electrode and monitoring the current. Most potentiostats available commercially today tend to be designed for use in laboratories and can be relatively bulky and expensive. They are, therefore, rather ill-suited for the purpose of this study.

A cheaper alternative, however, can be produced if the potentiostat is designed to be controlled by a low-cost embedded micro-controller. For this study, the STM32-F302R8 micro-controller board was used. Figure 15 shows the schematic of a potentiostat that was designed and manufactured on a printed circuit board (PCB). Prior to manufacturing, the PCB design was simulated and checked using LTspice, an analog electronic circuit simulator produced by Analog Devices. The PCB was manufactured by an external manufacturer and has the dimensions of 9cm x 5cm. The overall cost of the PCB, including components, was approximately £50.

Terminals X1-1 and X1-2 on the PCB are connected to +9V and -9V sources respectively, which, in this case, are provided by rechargeable 9V batteries. Terminal X1-3 is connected to the ground pin on the micro-controller. The op-amp C4 is a transimpedance amplifier which allows current to be converted into a voltage signal that can be measured by the micro-controller.

Since most micro-controllers are only capable of generating potentials of +0.0 to +3.3V, the op-amp array of C1, C2, and C3 is necessary to allow negative potentials to be produced. This is achieved by dividing the potential generated by the digital-to-analogue converter (V_{DAC}) on the micro-controller and amplifying it, using the +3.3V that is generated by the V_{out} pin as a reference (see Table 8).

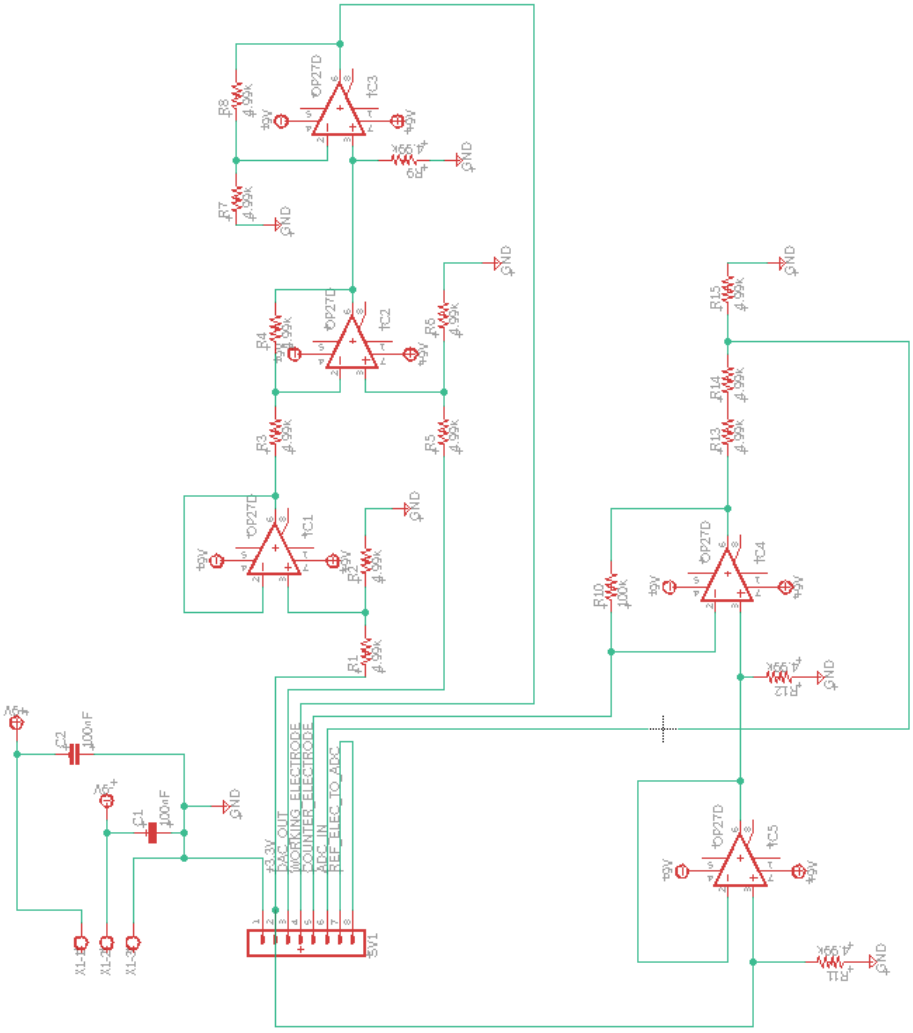

Figure 15: Potentiostat design, for use with the STM32-F302R8 microcontroller board

Table 8: Conversion of the +0.0 to +3.3V potential range generated by the micro-controller to a -3.3 to +3.3V range by the PCB potentiostat

V_{DAC}	V_{output}
+3.300V	+3.300V
+2.475V	+1.650V
+1.650V	+0.000V
+0.825V	-1.650V
+0.000V	-3.300V

4.1.2 Differential Pulse Anodic Stripping Voltammetry (DPASV)

The voltammetric method chosen for this study is anodic stripping voltammetry (ASV), using a differential pulse waveform for the potential scan during the stripping step. As discussed in Section 2.5.5, ASV is the most widely used technique for the determination of trace metals. The use of a differential pulse waveform should provide a more selective and sensitive measurement [7]. The analyte chosen for this study is zinc ion (Zn^{2+}), which was prepared by dissolving $Zn(NO_3)_2.6H_2O$ (Sigma-Aldrich) in deionised water.

The applied potential and waveform are generated by the potentiostat (Figure 15), which is controlled by a programmable embedded microcontroller (in this case, the STM32 Nucleo-F302R8 board). An accumulation potential of -2.9V (vs. C) was used at the deposition step for 75s. The differential pulse waveform at the stripping step had a step height of 10mV, pulse amplitude of 50mV, pulse repetition time of 0.2s, and pulse duration of 50ms. The potential was scanned from -2.9V to 0.0V during the stripping step.

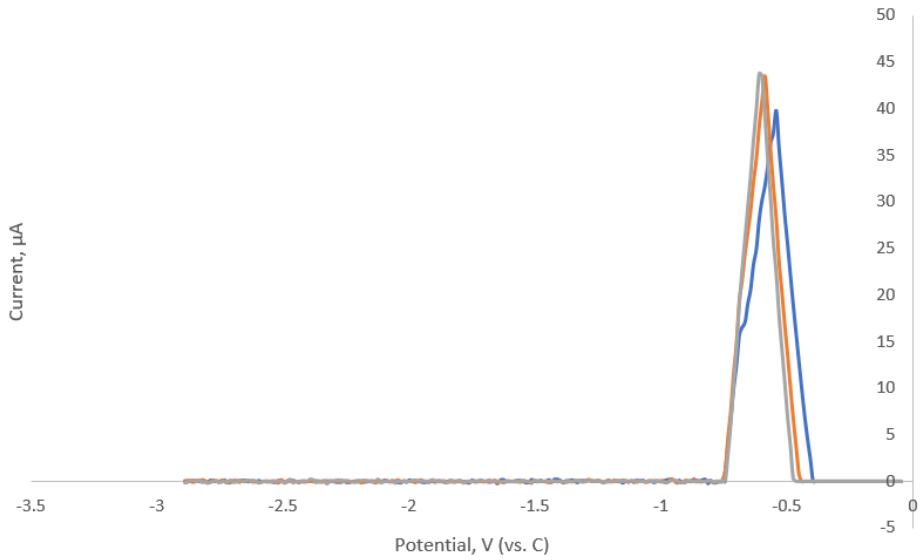

Figure 16: Typical differential pulse anodic stripping voltammogram obtained for 1.76g L^{-1} Zn^{2+} using a deposition potential of -2.9V (vs. carbon) and deposition time of 75s

Figure 16 shows a typical differential pulse stripping voltammogram for 1.76g L^{-1} Zn^{2+}, obtained by plotting the measured current against the stepped voltage as described in Section 2.5.5 and Figure 8. Figure 17 shows a plot of the peak currents (i_p) measured at a number of concentrations of Zn^{2+} within the range of 0.11 to 1.76g L^{-1}.

A well-defined stripping peak was obtained for 1.76g L^{-1} Zn^{2+} with a peak potential (E_p) of -0.6V (vs. C), and a fairly linear curve was obtained, which is promising. However, the sensor was unable to reliably measure Zn^{2+} concentrations of lower than 0.11g L^{-1}. This is a far-cry from matching the capability of conventional lab-based measurement techniques, which generally able to measure concentrations of approximately 800μg L^{-1} (parts-per-billion range) and lower.

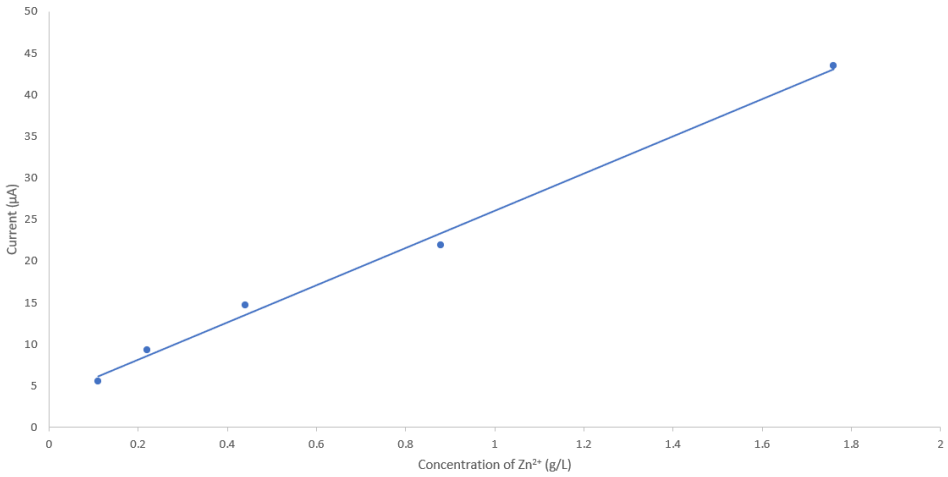

Figure 17: The peak current (i_p) vs. concentration curve obtained for 0.11 to 1.76g L^{-1} Zn^{2+}

4.2 Conclusions and Further Considerations for Future Designs

The work done in this section indicates that the use of pencil graphite electrodes and a PCB potentiostat for the determination of trace metals via DPASV is a promising idea and deserves further investigation. However, the concentration range of Zn^{2+} measured in this study (0.11 to 1.76g L^{-1}) is rather high compared to lab-based voltammetric methods which can measure concentrations of approximately 800μg L^{-1} (parts-per-billion range) and lower. Hence, further tests should be conducted for lower concentrations before comparing the performance of the pencil graphite electrodes and PCB potentiostat to standard lab-based equipment.

One obvious limitation of this design is the need for calibration curves (*i.e.* peak current vs. concentration), such as Figure 17, to be constructed before carrying out field tests for the desired analyte. The use of non-standard electrodes as well as a pseudo-reference electrode means that standard calibration curves are not very useful. Further designs should take this into account and careful consideration should be given as to whether the advantages in cost and portability of this design outweighs the need to construct calibration curves for each analyte.

There is also room for improvements and/or adjustments to be made on the PCB potentiostat design (Figure 15). For example, if a larger potential range than -3.3 to +3.3V is required, the gain on op-amp C3 can be increased by changing the values of resistors R7 and R8. The value of resistor R10 can also be increased to provide greater sensitivity of measurements.

5 Conclusions and Future Work

5.1 Temperature Sensing

The work done in Section 3 in integrating the temperature sensor onto the autonomous surface vehicle was successful in showing the ease at which sensor "payloads" can be mounted onto the vehicle. The study was also successful in demonstrating how autonomous missions can be customised and programmed for the autonomous surface vehicle.

5.2 Heavy Metals Sensing

In Section 4, the study was partially successful in realising the aim and the objectives outlined in Section 1.1. While the sensor and potentiostat were capable of measuring Zn^{2+} concentrations as low as 0.11g L^{-1}, conventional lab-based measurement techniques are able to measure concentrations of approximately 800μg L^{-1} (parts-per-billion range) and lower.

With an eye on both cost and portability, a compact and inexpensive PCB potentiostat, that is controlled by an embedded micro-controller board, was designed. Pencil graphite electrodes were also shown to be promising alternatives to standard voltammetric electrodes for the determination of Zn^{2+}, although further investigation is still needed on the electrodes' ability to measure minute concentrations of around 800μg L^{-1} (parts-per-billion range) and lower.

Further work should also be done with the pencil graphite electrodes for the measurement of other heavy metals, such as Cu and Hg, as well as the for the determination of multiple analytes at the same time. For this design to be viable, the electrodes need to be selective enough to produce well-defined peak potentials for each analyte when determining multiple analytes simultaneously.

References

[1] J. Fontes, "Temperature Sensors," in *Sensor Technology Handbook* (J. S. Wilson, ed.), ch. 20, pp. 531–561, Elsevier, 2005.

[2] C. N. Reddy, P. ReddyPrasad, and N. Sreedhar, "Electrochemical Analysis of Antichemotherapeutic Drug Zanosar in Pharmaceutical and Biological Samples by Differential Pulse Polarography," *Journal of Analytical Methods in Chemistry*, 2013.

[3] T. S. Cheng, M. Z. Mohamad Nasir, A. Ambrosi, and M. Pumera, "3-D printed metal electrodes for electrochemical detection of phenols," *Applied Materials Today*, vol. 9, pp. 212–219, 2017.

[4] J. Baron-Jaimez, M. R. Joya, and J. Barba-Ortega, "Anodic stripping voltammetry - ASV for determination of heavy metals," *Journal of Physics: Conference Series*, vol. 466, 2013.

[5] M. Amin, M. Mohd Isa, and R. Mohd Sidek, "An Embedded Processing of Differential Pulse Voltammetry (DPV) Data Using ARM processor (LPC1768)," in *IEEE International Circuits and Systems Symposium*, pp. 80–84, 2015.

[6] Y. Lattach, *Development and characterization of sensing layers based on molecularly imprinted conducting polymers for the electrochemical and gravimetrical detection of small organic molecules.* PhD thesis, 2011.

[7] K. C. Honeychurch, Z. Rymansaib, and P. Iravani, "Sensors and Actuators B : Chemical Anodic stripping voltammetric determination of zinc at a 3-D printed carbon nanofiber-graphite-polystyrene electrode using a carbon pseudo-reference electrode," *Sensors & Actuators: B. Chemical*, vol. 267, pp. 476–482, 2018.

[8] ArduPilot, "Pixhawk Overview," 2016.

[9] R. Desmarais and J. Breuer, "How to Select and Use the Right Temperature Sensors," *Sensors*, vol. 18, pp. 24–36, 2001.

[10] Maxim Integrated, "DS18B20 Datasheet," tech. rep., Maxim Integrated Products Inc., 2015.

[11] A. M. Volpe, B. K. Esser, and G. M. Bianchini, "Real-time ocean chemical measurement: at-sea ICP-MS experiments," *Journal of Analytical Atomic Spectrometry*, vol. 16, no. 8, pp. 801–805, 2001.

[12] European Union, "Directive 2000/60/EC of the European parliament and of the council of 23 October 2000 establishing a framework for

Community action in the field of water policy," *Official Journal of the European Communities*, 2000.

[13] F. Fornai, G. Ferri, A. Manzi, F. Ciuchi, F. Bartaloni, and C. Laschi, "An Autonomous Water Monitoring and Sampling System for Small-Sized ASVs," *IEEE Journal of Oceanic Engineering*, vol. 42, no. 1, pp. 1–8, 2016.

[14] T. H. Y. Tebbutt, *Principles of Water Quality Control*. Boston, MA: Butterworth-Heinemann, 5th ed., 1998.

[15] U. Löptien and H. E. Meier, "The influence of increasing water turbidity on the sea surface temperature in the Baltic Sea: A model sensitivity study," *Journal of Marine Systems*, vol. 88, no. 2, pp. 323–331, 2011.

[16] L. Råman Vinnå, A. Wüest, and D. Bouffard, "Physical effects of thermal pollution in lakes," *Water Resources Research*, vol. 53, pp. 3968–3987, may 2017.

[17] C. E. Raptis, J. M. Boucher, and S. Pfister, "Assessing the environmental impacts of freshwater thermal pollution from global power generation in LCA," *Science of the Total Environment*, vol. 580, pp. 1014–1026, 2017.

[18] C. E. Raptis and S. Pfister, "Global freshwater thermal emissions from steam-electric power plants with once-through cooling systems," *Energy*, vol. 97, pp. 46–57, feb 2016.

[19] R. B. Clark, *Marine Pollution*. Oxford: Oxford University Press, 5th ed., 2001.

[20] L. J. Vitt and J. P. Caldwell, "Water Balance and Gas Exchange," in *Herpetology*, ch. 6, pp. 181–202, Elsevier, 2013.

[21] M. Klavinš, A. Briede, V. Rodinov, I. Kokorite, E. Parele, and I. Klavina, "Heavy metals in rivers of Latvia," *Science of the Total Environment*, vol. 262, no. 1-2, pp. 175–184, 2000.

[22] R. Eisler, "Zinc Hazards to Fish, Wildlife, and Invertebrates: A Synoptic Review," *US Fish and Wildlife Service Contaminant Hazard Reviews*, vol. 26, no. 10, 1993.

[23] S. Edberg, E. Rice, R. Karlin, and M. Allen, "Escherichia coli: the best biological drinking water indicator for public health protection," *Journal of Applied Microbiology*, vol. 88, no. S1, pp. 106S–116S, 2000.

[24] C. J. Weiskerger and R. L. Whitman, "Monitoring E. coli in a changing beachscape," *Science of the Total Environment*, vol. 619-620, pp. 1236–1246, 2018.

[25] R. J. Diaz and R. Rosenberg, "Spreading Dead Zones and Consequences for Marine Ecosystems," *Science*, vol. 321, pp. 926–929, aug 2008.

[26] National Oceanic and Atmospheric Administration, "Are all algal blooms harmful?," 2018.

[27] G. Ferri, A. Manzi, F. Fornai, B. Mazzolai, C. Laschi, F. Ciuchi, and P. Dario, "Design, fabrication and first sea trials of a small-sized autonomous catamaran for heavy metals monitoring in coastal waters," in *Proceedings - IEEE International Conference on Robotics and Automation*, no. Vi, pp. 2406–2411, 2011.

[28] J. Curcio, J. Leonard, and A. Patrikalakis, "SCOUT - A Low Cost Autonomous Surface Platform for Research in Cooperative Autonomy," in *Proceedings of OCEANS 2005 MTS/IEEE*, pp. 1–5, IEEE, 2005.

[29] A. Pascoal, P. Oliveira, C. Silvestre, L. Sebastiao, M. Rufino, V. Barroso, J. Gomes, G. Ayela, P. Coince, M. Cardew, A. Ryan, H. Braithwaite, N. Cardew, J. Trepte, N. Seube, J. Champeau, P. Dhaussy, V. Sauce, R. Moitie, R. Santos, F. Cardigos, M. Brussieux, and P. Dando, "Robotic ocean vehicles for marine science applications: the European ASIMOV project," in *OCEANS 2000 MTS/IEEE Conference and Exhibition. Conference Proceedings (Cat. No.00CH37158)*, vol. 1, pp. 409–415, IEEE, 2000.

[30] J. Majohr and T. Buch, "Modelling, simulation and control of an autonomous surface marine vehicle for surveying applications Measuring Dolphin MESSIN," in *Advances in Unmanned Marine Vehicles* (G. N. Roberts and R. Sutton, eds.), ch. 16, pp. 329–352, Stevenage: Institute of Engineering and Technology, 2006.

[31] W. Naeem, T. Xu, R. Sutton, and J. Chudley, "Design of an unmanned catamaran with pollutant tracking and surveying capabilities," in *UKACC Control 2006 Mini Symposia*, vol. 2006, pp. 99–113, IEE, 2006.

[32] M. Dunbabin and A. Grinham, "Experimental evaluation of an Autonomous Surface Vehicle for water quality and greenhouse gas emission monitoring," in *2010 IEEE International Conference on Robotics and Automation*, pp. 5268–5274, IEEE, may 2010.

[33] M.-È. Garneau, T. Posch, G. Hitz, F. Pomerleau, C. Pradalier, R. Siegwart, and J. Pernthaler, "Short-term displacement of Planktothrix rubescens (cyanobacteria) in a pre-alpine lake observed using an autonomous sampling platform," *Limnology and Oceanography*, vol. 58, no. 5, pp. 1892–1906, 2013.

[34] M. Caccia, M. Bibuli, R. Bono, and G. Bruzzone, "Basic navigation, guidance and control of an Unmanned Surface Vehicle," *Autonomous Robots*, vol. 25, pp. 349–365, nov 2008.

[35] V. Vojinović, J. M. S. Cabral, and L. P. Fonseca, "Real-time bioprocess monitoring: Part I: In situ sensors," *Sensors and Actuators, B: Chemical*, vol. 114, no. 2, pp. 1083–1091, 2006.

[36] J. R. Leigh, *Temperature Measurement and Control*. London: Peter Peregrinus Ltd., 1988.

[37] W. Yantasee, Y. Lin, K. Hongsirikarn, G. E. Fryxell, R. Addleman, and C. Timchalk, "Review Electrochemical Sensors for the Detection of Lead and Other Toxic Heavy Metals : The Next Generation of Personal Exposure Biomonitors," *Environmental Health Perspectives*, vol. 115, no. 12, pp. 1683–1690, 2007.

[38] R. Kadara, N. Jenkinson, and C. Banks, "Disposable bismuth oxide screen printed electrodes for the high throughput screening of heavy metals," *Electroanalysis*, vol. 21, pp. 2410–2414, 2009.

[39] N. Serrano, J. Diaz-Cruz, C. Arino, and M. Esteban, "Stripping analysis of heavy metals in tap water using the bismuth film electrode," *Analytical and Bioanalytical Chemistry*, vol. 396, pp. 1365–1369, 2010.

[40] S. P. Kounaves, "Voltammetric Techniques," in *Handbook of Instrumental Techniques for Analytical Chemistry* (F. A. Settle, ed.), pp. 709–725, New Jersey: Prentice Hall PTR, 1997.

[41] R. L. McCreery, "Carbon electrodes: structural effects on electron transfer kinetics," in *Electroanalytical Chemistry* (A. J. Bard, ed.), vol. 18, New York: Marcel Dekker, 1991.

[42] K. Kalcher, J. M. Kauffmann, J. Wang, I. Svancara, K. Vytras, C. Neuhold, and Z. Yang, "Sensors based on carbon paste in electrochemical analysis: A review with particular emphasis on the period 1990-1993," *Electroanalysis*, vol. 7, no. 1, 1995.

[43] M. E. Rice, Z. Galus, and R. N. Adams, "Graphite paste electrodes: Effects of paste composition and surface states on electron-transfer rates," *Journal of Electroanalytical Chemistry and Interfacial Electrochemistry*, vol. 143, no. 1-2, pp. 89–102, 1983.

[44] A. M. Bond, P. J. Mahon, J. Schiewe, and V. Vicente-Beckett, "An inexpensive and renewable pencil electrode for use in field-based stripping voltammetry," *Analytica Chimica Acta*, vol. 345, pp. 67–74, 1997.

[45] D. Blum, W. Leyffer, and R. Holze, "Pencil-Leads as new electrodes for abrasive stripping voltammetry," *Electroanalysis*, vol. 8, no. 3, 1996.

[46] W. Gao, J. Song, and N. Wu, "Voltammetric behavior and square-wave voltammetric determination of trepibutone at a pencil graphite electrode," vol. 576, pp. 1–7, 2005.